

IC 4329A: THE NEAREST QUASAR?

A. S. WILSON

Astronomy Centre, University of Sussex; and Astronomy Program, University of Maryland

AND

M. V. PENSTON

Anglo-Australian Observatory; and Astronomy Division, ESTEC, ESA Villafranca Satellite Tracking Station

Received 1979 January 8; accepted 1979 March 5

ABSTRACT

A spectrophotometric study of the Seyfert galaxy IC 4329A has been made with the Anglo-Australian Telescope. Fe II emission is found in the spectrum as well as forbidden lines with ionizations ranging up to [Fe X] $\lambda 6374$. The Balmer lines are double peaked, the secondary (more highly redshifted) component having a flatter Balmer decrement than the main one. The equivalent widths of most lines seem to be variable, with changes in the continuum level being the most plausible explanation.

That the nucleus of IC 4329A is heavily reddened is indicated by the facts that (i) a prominent dust lane is seen to bisect the nucleus, (ii) the Balmer decrement ($H\alpha/H\beta \approx 12$) is steeper than found in any other Seyfert galaxy, (iii) the observed nuclear optical continuum is very steep ($F_\nu \propto \nu^{-4.4}$), and (iv) prominent Na I D-line absorption is seen at the redshift of IC 4329A. The values of A_v derived from (ii), (iii), and (iv) above are 4.8, 2.5, and > 1.6 mags, respectively. If A_v lies in the range 2.5–4.8 mag, as seems most likely, the absolute nuclear magnitude M_v lies in the range -23.0 to -25.3 , values typical of quasars. The observations of the Na I D lines have also been used to deduce that the velocity dispersion of the absorbing sodium atoms lies in the range 8.4 – 13.5 km s $^{-1}$ with 90% confidence. This small dispersion suggests that noncircular motions in the disk of IC 4329A are small and that the velocity dispersion of its interstellar medium is quite comparable to that in our Galaxy, contrary to theoretical speculations that the interstellar medium in Seyferts might be seriously disrupted.

Subject headings: galaxies: Seyfert — galaxies: structure — quasars

I. INTRODUCTION

The Seyfert nature of the galaxy IC 4329A was discovered by A. R. Sandage in a redshift survey of southern galaxies with the Mount Stromlo 74 inch (1.8 m) telescope (see Disney 1973). Further studies were made by Disney (1973) and Martin (1974). Disney described the object as “an extreme Seyfert galaxy” on account of the width of $H\alpha$ ($\sim 13,000$ km s $^{-1}$) and the high $H\beta$ luminosity. The galaxy is an edge-on spiral close to the giant elliptical IC 4329, which is the brightest galaxy in a rich cluster of ellipticals and spirals in the Centaurus region.

In this paper, we report a more detailed spectrophotometric study of the nucleus of IC 4329A with the Anglo-Australian Telescope. In § 2 we describe the observations and their reduction, while in § 3, we discuss the emission-line intensities, their widths and structures, possible variability, and the shape of the continuum. In § 4 we consider the absorption to the nucleus, while in § 5 we emphasize that the nuclear luminosity is, after correction for visual absorption, typical of lower-luminosity quasars.

II. SPECTROSCOPIC OBSERVATIONS

Eight spectra of the nucleus of IC 4329A were obtained with the Anglo-Australian Telescope (3.9 mag.

The dates of observation, integration times, and other relevant parameters are listed in Table 1.

The detector for observations 1, 2, and 3 was the Image Dissector Scanner (IDS; Robinson and Wampler 1972, 1973). The first and second of these employed a spectrograph borrowed from the Lick Observatory mounted at the f/8 Cassegrain focus. The grating had 600 lines mm $^{-1}$ and was used in the first order. For the third observation, the Boller and Chivens “Fast Spectrograph” was mounted at the f/15 Cassegrain focus. The grating was used in the first order and had 1200 lines mm $^{-1}$. Full descriptions of the observational and reduction procedures, including sky subtraction and wavelength calibration, have been given elsewhere (Robinson and Wampler 1972, 1973). The sensitivity of the instrument as a function of wavelength was determined by observations of the photometric standard stars W485A and L745–46A (Oke 1974).

The remaining five observations (4–8) used the Image Photon Counting System (IPCS; Boksenberg 1972; Boksenberg and Burgess 1973) attached to a spectrograph constructed at the Royal Greenwich Observatory and mounted at the f/8 Cassegrain focus. Observations 5, 6, 7, and 8 used grating 1 (1200 lines mm $^{-1}$); observation 4 employed grating 3 (270 lines mm $^{-1}$).

TABLE 1
OBSERVATIONS AND SYSTEM PARAMETERS

OBSERVATION NUMBER	DATE	SPECTROGRAPH	DETECTOR	WAVELENGTH COVERAGE (Å)	RESOLUTION FWHM (Å)	INTEGRATION (min)	OBJECT AND SKY APERTURES		
							Size (arcsecs)	Separation (arcsecs)	Figure No.
1.....	1975 June 9/10	Lick	IDS	3380-6000	10	32	3 × 6	30	...
2.....	1975 June 10/11	Lick	IDS	4820-7400	10	32	3 × 6	30	2a
3.....	1976 March 0/1	Boller and Chivens	IDS	3700-5120	5	48	1.8 × 4.5	20	1
4.....	1977 June 13/14	RGO	IPCS	4500-8000	5	33	1.3 × 4.7	14	2b
5.....	1977 June 24/25	RGO	IPCS	4830-5170	0.5	67	1.3 × 2.8	10	3
6.....	1977 July 19/20	RGO	IPCS	6000-6980	1.5	67	1.3 × 4.7	14	4
7.....	1977 July 30/31	RGO	IPCS	5260-6200	1.5	67	1.3 × 6.2	12	...
8.....	1977 August 23/24	RGO	IPCS	5840-6140	0.5	67	0.6 × 2.4	5	6

With the 82 cm camera, grating 1 gives 10 \AA mm^{-1} (observations 5 and 8), while with the 25 cm camera the dispersion becomes 30 \AA mm^{-1} (observations 6 and 7). Observation 4 was obtained with the 25 cm camera at 130 \AA mm^{-1} . All the IPCS observations were sky subtracted, wavelength calibrated, and "scrunched," i.e., the width of the individual spectral channels was adjusted to be a fixed wavelength interval and the counts per channel modified accordingly. However, only the low-dispersion spectrum (observation 4) was reduced to intensity units through observations of W485A. The high-dispersion spectra are presented as counts per channel against wavelength.

III. RESULTS

a) Redshift

The heliocentric redshifts, along with their rms errors, of the various types of lines exhibited by IC 4329A are as follows:

z_h (Na I D-line absorption)	$= 0.016140 \pm 0.00003$
z_h (Ca II K and Mg I b absorption)	$= 0.01605 \pm 0.0006$
z_h (peaks of Balmer lines)	$= 0.01588 \pm 0.0002$
z_h ([O III])	$= 0.01606 \pm 0.0001$
z_h ([O I], [O II], [S II])	$= 0.01576 \pm 0.0002$

The greatest discrepancy between these different systems concerns the Na I D absorption and the low-excitation forbidden lines. This difference however, is only 1.9σ and probably not significant. Our best value

for the redshift of IC 4329A with reference to the galactic center is $0.01567 \pm 0.0001 = 4697 \pm 30 \text{ km s}^{-1}$ (from the Na I D-line absorption).

b) Line Intensities

Figures 1 and 2 show low-dispersion spectra of IC 4329A, in the form of relative intensity ($= F_\lambda \times \text{constant}$). The relative intensity at different wavelengths in these diagrams should be reliable to better than 20%. The stronger lines are marked, as are the Fe II multiplets which are present. The relative intensities of the lines within each multiplet (as given by Moore 1972) are also indicated.

Table 2 presents a list of intensities of the detected emission and absorption lines relative to $H\beta$, both as observed and after correction for the reddening corresponding to $A_v = 4.8$ mag, which is derived later from the Balmer decrement (§ IV a). Note that higher-dispersion data, discussed later, have been used to separate lines blended in the low-resolution spectra. For the stronger lines, the relative intensities should be good to 20% or better, but the errors increase for weaker lines where noise becomes important. The intensities found by Disney (1973) and Martin (1974) for the stronger lines are also listed in Table 2. For 50% of the lines, our values agree with Disney's to better than 10%. The discrepancies are that our Balmer decrement is steeper than Disney's and that the present data indicate [O I] $\lambda 6300.2$ to be a factor of 3.6 smaller than he found. The agreement between our data and Martin's is also good except for [O II] $\lambda 3727.5$ and He I $\lambda 5875.6$.

c) Emission-Line Spectrum—Detailed Discussion

Most of the lines visible in Figures 1 and 2 and listed in Table 2 are common features of the spectra of

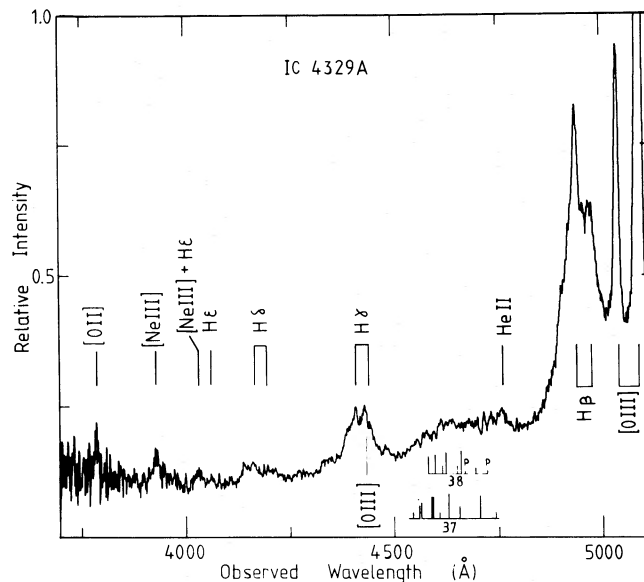


FIG. 1.—Spectrum of the nucleus of IC 4329A from $\lambda 3700$ to $\lambda 5120$ taken with the Image Dissector Scanner on 1976 March 0/1. The laboratory wavelengths and relative intensities within the observed Fe II multiplets (37 and 38) are given. For lines marked *P*, the wavelength is predicted from the laboratory term values. For further details, see § II and Table 1.

TABLE 2
LINE INTENSITIES IN IC 4329A

Rest Wavelength Å	Identification	Relative Intensity (this paper)	Number of Independent Estimates of Intensity Averaged to Give Previous Column	Relative Intensity (Disney 1973)	Relative Intensity (Martin 1974)	Relative Intensity Corrected for Reddening	Comments
3727.5	[OII]	1.8	2	2	10	11.8	
3868.7	[NeIII]	1.5	2			7.3	
3888	HeI+H8	0.8	1			3.7	
3933.7	CaII	2.0Å	1			4.3	Absorption, equivalent width given
3969	[NeII]+Hc	1.0	1			4.0	
4068.6 + 4076.2	[SII]	1.1	2			3.6	
4101.7	Hδ	4.2	2	9		13.2	
4340.5	Hγ	13.6	2	26	20	28.6	
4363.2	[OIII]	1.1-3.6*	2	1.5-4.5		2.2-7.3*	Separation Unsure
4541.6	HeII	0.7:	1			1.1	Could be FeII
4570	FeII(37+38)	22*	2			32.6*	
4658.1	[FeIII]	0.5	1			0.7	
4685.7	HeII	1.6	2			2.0	
4861.3	Hβ	100	4	100	100	100	
4958.9	[OIII]	20.0	4	20	20	17.7	
5006.8	[OIII]	64.7	4	66	64	54.0	
5158.3	[FeVII]	1.7:	2			1.1:	Could be FeII
5183.6	MgI	0.6Å	2			0.3	Absorption, equivalent width given
5300	FeII(48+49)	31*	3			18*	
5720.9	[FeVII]	5.1	2			2.0	
5875.6	HeI	42	2	46	12	14.5	
5893	NaI	2.18Å	2			2.7	Absorption, equivalent width given
6085.5	[FeVII]	3.9	2			1.1	
6300.2	[OI]	4.4	2	16	4	1.1	
6374	[FeX]	3.3*	2			0.8*	
6548.1	[NII]	1160	2	817	780	233	
6562.8	Hα	20*	1	8		4*	
6583.6	[NII]	8.6*	1	25	25	1.6*	
6717.0	[SII]	13.0*	1			2.4*	

NOTES TO TABLE 2

NOTE.—Colon indicates doubtful reality of identification.

* These intensities are uncertain because of either blending with adjacent lines or difficulty in defining the continuum level.

Type 1 Seyfert galaxies. The Balmer series dominates the spectrum, and forbidden lines from species with a wide range in ionization—[O I] to [Fe VII] and [Fe X]—are detected. In the present subsection, some of the important features are discussed in some detail.

i) Fe II Emission

It is now clear that Fe II emission is found in most Type 1 Seyferts (Osterbrock 1977), although its intensity relative to the Balmer lines varies greatly from galaxy to galaxy. The spectra of some objects, such as I Zw 1 (Phillips 1976) and Markarian 231 (Boksenberg *et al.* 1977), are dominated by lines of Fe II and the Balmer series. In most galaxies, however, Fe II is much weaker and manifests itself as two very broad features, one between $H\gamma$ and $H\beta$ and the other centered near $\lambda 5300$. These broad features, visible in IC 4329A, are the result of blending of closely spaced,

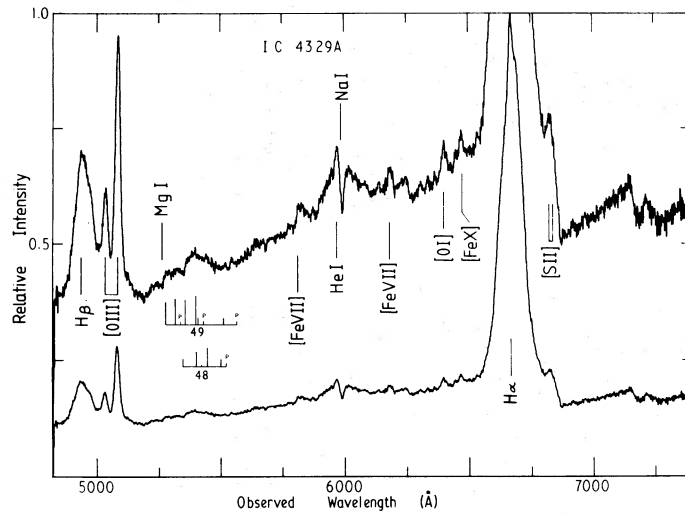


FIG. 2a

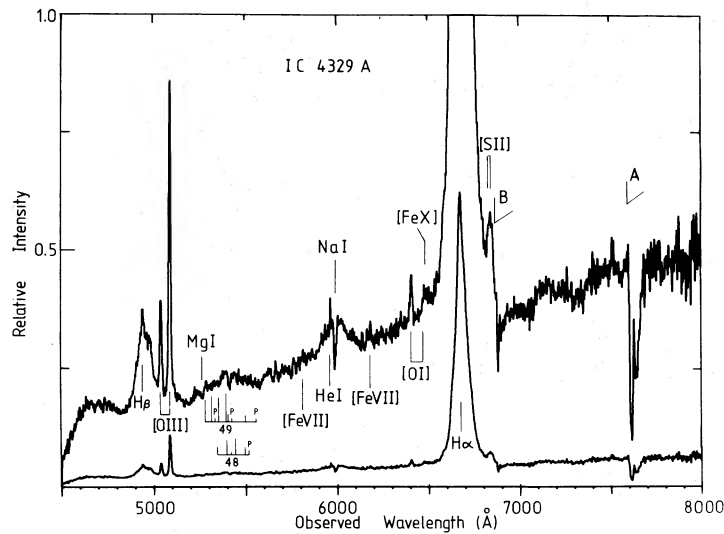


FIG. 2b

FIG. 2.—Spectra of the nucleus of IC 4329A. In each diagram, the two plots represent the same data plotted with a different intensity scale but the same zero. The upper plot enables weak features to be seen more easily. The laboratory wavelengths and relative intensities *within* the observed Fe II multiplets (48 and 49) are given. For lines marked P, the wavelength is predicted from the laboratory term values. (a) Spectrum from $\lambda 4820$ to $\lambda 7400$ taken with the Image Dissector Scanner on 1975 June 10/11. The resolution (FWHM) is 10 Å. (b) Spectrum from $\lambda 4500$ to $\lambda 8000$ taken with the Image Photon Counting System on 1977 June 13/14. The resolution (FWHM) is 5 Å. For further details, see § II and Table 1.

broad lines of Fe II occurring in a number of multiplets. We searched our spectra of IC 4329A, therefore, for all multiplets of Fe II detected by Phillips (1976) in I Zw 1 and found multiplets 37, 38, 48, and 49 (see Figs. 1 and 2). The weak, broad feature centered near rest wavelength 5162 Å may be ascribed to either [Fe VII] λ 5158.3 or Fe II λ 5169.03 of multiplet 42. The peak of the broad Fe II feature redward of H β at a rest wavelength 5314.8 Å is probably dominated by Fe II λ 5316.8 (multiplet 48) and Fe II λ 5316.6 (multiplet 49), although a contribution from [Ca V] λ 5308.9 cannot be ruled out. It should be emphasised that the observed intensities of the two Fe II blends, as listed in Table 2, are quite uncertain because of difficulty in defining the level of the local continuum. This uncertainty may amount to $\pm 50\%$.

ii) [Fe x] Emission

Of interest is the probable detection of the coronal line [Fe x] λ 6374 in IC 4329A. As in other Seyfert galaxies (Cooke *et al.* 1976; Osterbrock 1977; Penston *et al.*, in preparation), this line is partially blended with [O I] λ 6363.9. However, the intensity ratio of the [O I] lines $I(6363.9 \text{ \AA})/I(6300.2 \text{ \AA})$ is fixed by atomic transition probabilities to be 0.32 (e.g., Osterbrock 1974, p. 52), so that the intensity of [Fe x] λ 6374 was taken to be the intensity of the blended feature minus 0.32 times the intensity of [O I] λ 6300.2.

Osterbrock (1977) ascribed this feature in several galaxies to a line of Fe II λ 6369.4, multiplet 40. However, the other lines of this multiplet, at λ 6432.7, 6516.1, have not been reported in any of these galaxies. According to Moore (1972), the laboratory intensity of these two lines is greater than the intensity of λ 6369.4 by factors of 2 and 5, respectively. However, the intensity of λ 6432.7 is observed to be < 0.7 times the intensity of λ 6370 in IC 4329A; as in most Type 1 Seyferts, λ 6516.1 is masked by the wing of H α . Thus either the relative intensities of the lines of multiplet 40 in IC 4329A deviate strongly from the values given in Moore (1972) or the line near λ 6370 cannot be ascribed to Fe II.

Identification of this feature with [Fe x] λ 6374 is of particular interest in view of the detection of X-ray emission from IC 4329A (Elvis *et al.* 1978; Delvaile, Geller, and Schnopper 1978). A discussion of the general properties of this line in Seyferts and any possible relationship to the X-ray emission is given elsewhere (Penston *et al.*, in preparation).

iii) Width and Structure of Emission Lines

Table 3 tabulates both the full width at half-maximum (FWHM) and the full width at zero intensity (FWOI) of some of the more prominent emission lines.

These values should be treated with some caution, since the FWHM depends to some extent on the detector resolution, especially when the line shows structure, and the FWOI on the signal-to-noise ratio in the line wing and the exact choice of continuum level. However, except where additional uncertainty is indicated, the individual values are probably good to $\pm 10\%$. For example, the result that $\text{FWOI}(\text{H}\alpha) > \text{FWOI}(\text{H}\beta)$ is presumably to be ascribed to the much greater strength of H α and the consequent better signal-to-noise ratio in the line wings. On the other hand, that the $\text{FWHM}(\text{H}\beta \text{ and } \text{H}\gamma) > \text{FWHM}(\text{H}\alpha)$ is probably a consequence of the second component seen in the profiles of H β and H γ (and also H δ and H ϵ) but not in H α (see Figs. 1, 2, 3, and 4 for the Balmer-line structure). This second peak, also noted by Disney (1973), has redshift $z_h = 0.0224$ (H ϵ), 0.0226 (H δ), 0.0227 (H γ), and 0.0221 (H β), with mean $z_h = 0.0224 \pm 0.0001$. A very weak feature, of questionable reality, at an observed wavelength 4790.1 Å could be identified with He II λ 4685.7 at $z = 0.0223$, the same as for the Balmer lines within the errors. There is evidence of additional structure in the Balmer lines, particularly in H β and the wings of H γ , but a detailed inter-comparison of their profiles is rendered difficult by differing spectral resolutions or by blending with adjacent lines. However, the Balmer decrement H α /H β is much steeper for the main component than for the secondary one (see Fig. 5).

Although the red wing of He I λ 5875.6 is mutilated by the strong Na I λ 5893 absorption, it is clear that its FWOI is comparable to that of the Balmer lines. [O III] λ 4958.9 and 5006.8 are considerably narrower and smoother (Fig. 3, Table 3).

iv) Variability

Variability of emission lines or continuum in galactic nuclei is of fundamental importance in delineating the extents of the various emitting regions, which may be too small for direct resolution. Inspection of our spectra yields the following tentative evidence for variability

1. Comparison of the two low-dispersion blue spectra (observations 1 and 3) shows that the *equivalent*

TABLE 3
WIDTHS OF THE STRONGER EMISSION LINES

Width	H α	H β	H γ	Mean of Balmer Lines	He I	[O III]
FWHM (km s^{-1}).....	3500	4600	4100	4070 ± 300	490
FWOI (km s^{-1}).....	15600	14600:	11900 ^a	14030 ± 1100	12900	1890

NOTE.—Colon indicates uncertainty due to blending with [O III] λ 4958.9.

^a Uncertain because of low signal-to-noise ratio in line wings.

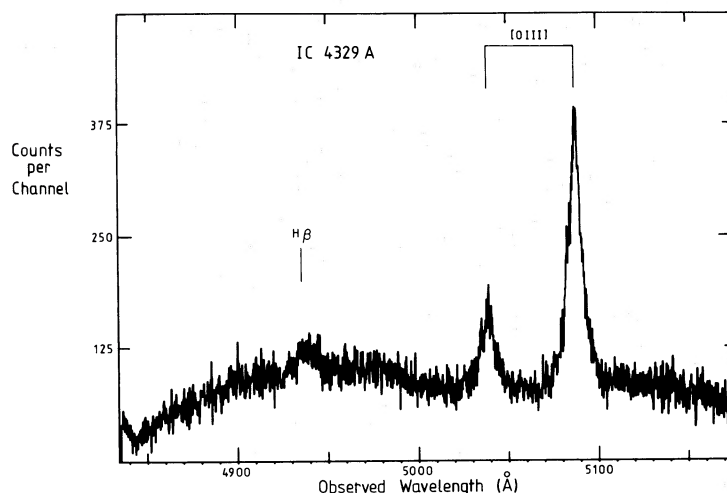


FIG. 3.—Region of $H\beta$, $[O\ III]\ \lambda\lambda 4858.9$ and 5006.8 in IC 4329A observed with the Image Photon Counting System on 1977 June 24/25. The resolution (FWHM) is $0.5\ \text{\AA}$.

widths of all lines are greater by a factor of ~ 2 in the 1976 March 0/1 observation than on 1975 June 9/10, although there is little or no change in the *intensities* of the stronger lines relative to $H\beta$.

2. Similarly, comparison of the two low-dispersion red spectra (observations 2 and 5) shows generally greater equivalent widths on 1977 June 13/14 than on 1975 June 10/11. A notable exception is the Na I D-line absorption $\lambda 5893$, whose equivalent width changed by less than 5% between these observations.

3. The apparent variability of emission-line equivalent width and the lack of change in line intensity relative to $H\beta$ are well illustrated by the $H\beta$, N1, N2 region for which five independent measurements are available. The equivalent widths and relative intensities are listed in Table 4. The simplest explanation of

these effects is a change in the continuum level. These results favoring variability should be considered preliminary since the observations were not obtained with the same spectrograph/detector system. In particular, it is conceivable that differing slit size could account for some or all of the above effects, although the equivalent widths of Table 4 do not seem to be correlated with aperture size. Monitoring with a large entrance aperture scanner with the same spectrograph would be well worthwhile.

d) Continuum Radiation

The continuum derived from the low-dispersion IDS data (obtained through a $3'' \times 6''$ aperture) may

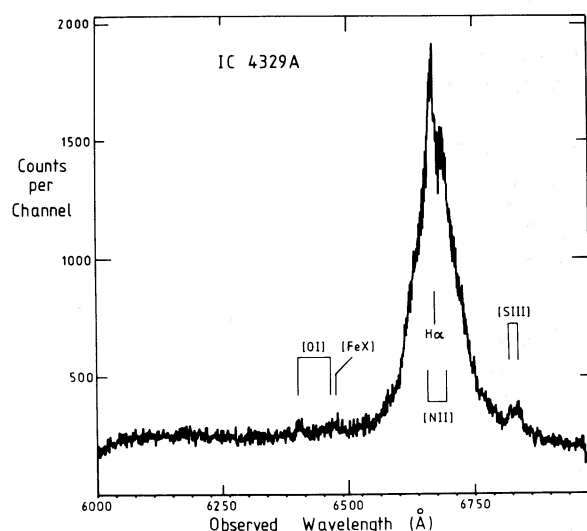


FIG. 4.—Spectrum of the nucleus of IC 4329A from $\lambda 6000$ to $\lambda 6980$ obtained with the Image Photon Counting System on 1977 July 19/20. The resolution (FWHM) is $1.5\ \text{\AA}$.

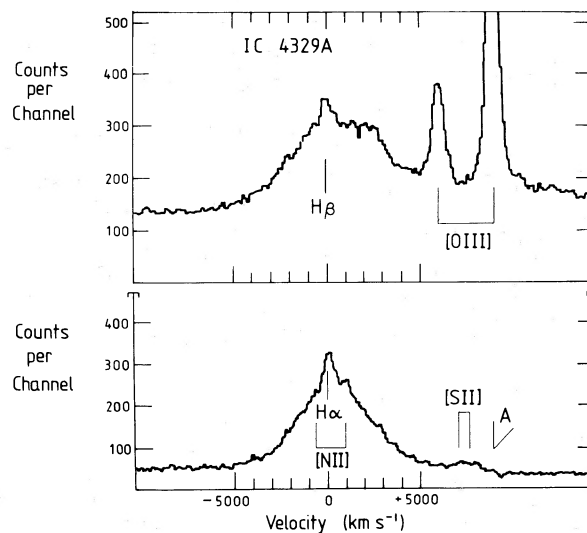


FIG. 5.—Comparison of the profiles of $H\beta$ (upper plot) and $H\alpha$ (lower plot) on the same velocity scale. Note the shoulder 1000 – $3000\ \text{km s}^{-1}$ to the red of the peak of $H\beta$, which is not seen in $H\alpha$.

TABLE 4
EQUIVALENT WIDTHS AND INTENSITIES RELATIVE TO H β

Line	1975 June 9/10	1975 June 10/11	1976 March 0/1	1977 June 13/14	1977 June 24/25
Equivalent Widths (Å)					
H β	103	74	253	109	...
[O III] λ 4958.9.....	18	15	57	21	12
[O III] λ 5006.8.....	59	42	188	71	36
Intensities Relative to H β = 100					
H β	100	100	100	100	...
[O III] λ 4958.9.....	18	20	23	20	...
[O III] λ 5006.8.....	60	57	74	68	...

be described to better than 20% over the range 3700 Å–6100 Å by a power law $F_\nu \propto \nu^{-\alpha}$ with $\alpha = 4.48 \pm 0.4$. The continuum of the IPCS low-dispersion spectrum (aperture $1''.3 \times 4''.7$) is well fitted with $\alpha = 4.32 \pm 0.3$ from 4800 Å–7900 Å. UVV photometry in a 10" diaphragm $V = 14.44$, $B - V = 0.96$, $U - B = 0.51$) published by Disney (1973) is broadly consistent with these values (ignoring the presence of emission lines in the filter bands), although the implied value of α is smaller between V and B and larger between B and U than the values derived above.

IV. REDDENING AND PHYSICAL CONDITIONS

The Balmer decrement in IC 4329A is steeper than expected if the lines are formed via normal recombination and downward cascading (case B conditions). Such a result is commonly found in Seyfert galaxy spectra. In a study of 36 Type 1 Seyfert galaxies, Osterbrock (1977) has shown that the observed $H\alpha/H\beta/H\gamma$ line ratios cannot, in general, be accounted for by intrinsic case B recombination values together with any chosen amount of interstellar extinction, assuming this extinction obeys the Whitford (1958) reddening law. He suggests that the Balmer decrement is intrinsically steeper than expected under case B conditions, presumably because of collisional excitation or self-absorption in the Balmer lines.

Despite these considerations, it is clear that the nucleus of IC 4329A is heavily obscured by dust because: (a) the Balmer decrement ($H\alpha/H\beta = 12$, $H\gamma/H\beta = 0.14$) is *very* steep, steeper than in any of the 36 optically selected Seyfert galaxies studied by Osterbrock (1977); (b) the continuum is also very steep ($F_\nu \propto \nu^{-4.4 \pm 0.3}$, § III); (c) prominent Na I D-line, and possibly other interstellar absorption features, are seen at the redshift of IC 4329A; and (d) the galaxy is a spiral viewed almost edge-on, with a prominent dust lane crossing the nucleus. Points (a), (b), and (c) may be used to give quantitative estimates of A_v , as we now show.

a) The Balmer Decrement

The reddening has been estimated in two ways, by assuming that either (i) the intrinsic Balmer decrement

is described by case B conditions at $T_e = 10000$ K, i.e., $H\alpha/H\beta = 2.87$, $H\gamma/H\beta = 0.466$, $H\delta/H\beta = 0.256$ (see Osterbrock 1974, p. 66) or (ii) the intrinsic Balmer decrement is the average of the values found by Osterbrock (1977) for 36 Type 1 Seyferts, i.e., $H\alpha/H\beta = 3.58$, $H\gamma/H\beta = 0.41$. Under assumption (i), $E_{B-V} = 1.89 \pm 0.2$ is found, or, taking $A_v = 3.0E_{B-V}$ (Allen 1972), $A_v = 5.7 \pm 0.7$ mag. Assumption (ii) leads to $A_v = 4.8 \pm 1$ mag. These estimates may be compared with the value $A_v = 4.2$ mag found by Disney (1973) from his data and assumption (i). After correction for $A_v = 4.8$ mag, the line intensities are as given in column (7) of Table 2. These estimates of A_v should be treated with caution since, as may be seen from Table 2, the de-reddened Balmer decrement is not in good agreement with the assumed intrinsic value, i.e., $H\alpha/H\beta$ is flatter than assumed and $H\gamma/H\beta$ steeper. This suggests that either the reddening law in IC 4329A is different to its galactic form or the intrinsic Balmer decrement is not as we have assumed. Also, because the observed Balmer decrement is a function of velocity (§ IIIc[iii]), both assumptions (i) and (ii) must be, at best, idealizations, i.e., the observations cannot be accounted for by any constant intrinsic decrement along with a fixed reddening.

b) The Continuum Radiation

If it is assumed that the intrinsic slope of the nuclear continuum is typical of Type 1 Seyferts, the reddening may be derived. Using the law $A_\lambda = 0.68A_v[(1/\lambda) - 0.35]$ mag (λ in μ) to correct the observed continuum, $A_v = 2.0$ mag yields a spectrum quite closely following the power law $F_\nu \propto \nu^{-1.9}$. Taking $A_v = 3.0$ mag yields a much flatter spectrum which is only poorly fitted by the best-fitting power law $F_\nu \propto \nu^{-0.7}$. Since the optical continuum slopes α of other Seyferts are typically in the range 0.5–1.5, the continuum is probably reddened by $A_v \approx 2.5 \pm 0.5$. We note that the fact that the Na I D-absorption lines are essentially black at their centers (see § IVc) implies that very little starlight originates from the *near* side of the obscuring material.

If the Balmer lines are formed as in normal radiative recombination theory, the slope of the (assumed power law) continuum in the ultraviolet can be derived from

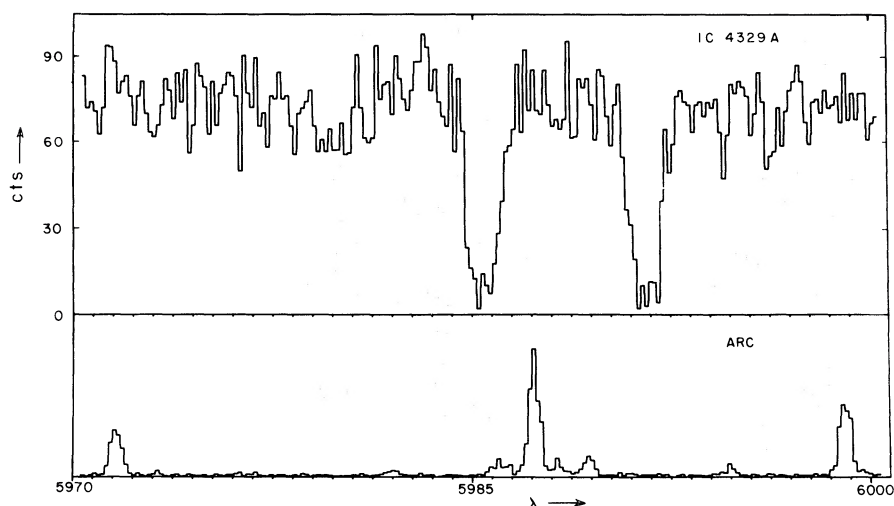


FIG. 6.—Spectrum of the nucleus of IC 4329A at 10 \AA mm^{-1} covering the region of the Na I D lines obtained on 1977 August 23/24 (*upper plot*) and the corresponding arc spectrum (*lower plot*). The data have been sky-subtracted and scrunched: approximate counts are plotted against observed wavelength. Comparison with the arc spectrum shows that the lines are well resolved with full widths at half the continuum intensity $\sim 72 \text{ km s}^{-1}$. Note the near-equal equivalent widths indicating saturated absorption by a large column density of sodium atoms in the Seyfert galaxy.

the observed equivalent width of $H\beta$. Using equation (A3) of Penston and Fosbury (1978), the $H\beta$ equivalent widths of 74–253 Å (Table 4) correspond to values of α in the range $+0.1$ – $+1.0$, depending on the exact choice of cut-off frequency for the ionizing continuum, values which substantiate the intrinsic optical continuum slope assumed above.

c) Na I D-Line Absorption

In order to obtain a further estimate of the amount of interstellar material in IC 4329A along the line of sight to its nucleus, detailed observations of the sodium D-line absorptions were undertaken (observations 7 and 8, see Table 1). The higher dispersion data are illustrated in Figure 6. It is seen that both D lines are clearly present in absorption, are of about equal equivalent width, and are spectrally resolved. The lines are essentially black in their centers if some allowance is made for the faint wings seen on most arc lines. As noted in § III, the mean radial velocity as measured from the two lines on the high-dispersion

data is $4842.1 \pm 9 \text{ km s}^{-1}$ with respect to the Sun, showing that the absorption indeed arises in IC 4329A, presumably in the dust lane seen to bisect the galaxy and cross the nucleus. The full widths of the lines at the half-continuum points are $72.1 \pm 2.1 \text{ km s}^{-1}$. The equivalent widths of the D lines and their ratios as measured from both spectra are given in Table 5. The equivalent widths are measured directly from the number of photons counted in the spectra as a function of channel number. The errors are computed by combining the Poissonian errors from the number of photons recorded in star and sky channels of the spectra with that made in defining the continuum, as found from the deviations of the nearby continuum about its mean level. Note that, although the actual values of the equivalent widths in the two spectra differ by more than their internal errors (presumably because of either the differing slit widths or differing amounts of scattered light in the two spectrograph cameras), the D-line ratios are in excellent agreement and there is every reason to believe that the errors in the ratios given in the table represent the total error (both internal and systematic).

TABLE 5
D-LINE EQUIVALENT WIDTHS AND STANDARD ERRORS

DATE OF SPECTRUM	DISPERSION \AA mm^{-1}	EQUIVALENT WIDTH		LINE RATIO D_2/D_1
		$\lambda 5890 (D_2)$	$\lambda 5896 (D_1)$	
1977 Aug. 23	10	1.22 ± 0.06^a	1.19 ± 0.06^a	1.021 ± 0.072
1977 July 30	30	0.92 ± 0.07^a	0.94 ± 0.07^a	0.976 ± 0.108
Unweighted mean		1.07 ± 0.15	1.07 ± 0.12	0.998 ± 0.065
Weighted mean		1.09 ± 0.15	1.09 ± 0.12	1.007 ± 0.060

^a Internal errors only.

The measured values of the D_2 equivalent width and the ratio D_2/D_1 may be analyzed by the method of Strömberg (1948) to yield the column density N of neutral sodium atoms responsible for the absorption and the parameter b which describes the velocity dispersion of those atoms. Because the lines are heavily saturated and their ratio essentially unity, attention must be paid to the portions of the curves of growth in which the equivalent widths are dominated by the natural damping, in order to establish an upper limit to the column density. The ratio D_2/D_1 is expected to be 2 in the linear (unsaturated) regime, to decrease to near 1 in the logarithmic (saturated) regime, and to approach $\sqrt{2}$ in the damping regime of the curves of growth. In fact, the minimum ratio predicted by theory is ~ 1.05 , consistent with the measured ratio 1.007 ± 0.060 . However, because the actual measured ratio (1.007) cannot be attained theoretically and because of the extreme nonlinearity of the predicted values of equivalent width and line ratio with N and b , the methods advocated by Lampton, Margon, and Bowyer (1976) have been used to find the acceptable ranges for these latter parameters.

In the present case, this method involves comparing (by means of a χ^2 test) the observationally determined equivalent width of D_2 and the doublet ratio (which were regarded as the independently observed parameters because it is believed that the line ratio is not subject to any systematic errors), and their errors with the corresponding values calculated theoretically as a function of b and N . These theoretical values were computed by D. C. Morton (private communication) using a Gaussian velocity profile [radial-velocity distribution function $\propto \exp(-v^2/b^2)$] and the f -values and damping constant of Morton and Smith (1973). The minimum value of χ^2 ($= \chi_{\min}^2$) is found to be 0.8 at the "best" values $b = 9.8 \text{ km s}^{-1}$ and $N = 2.5 \times 10^{15} \text{ cm}^{-2}$. No exact fit is possible since the theoretical doublet ratio cannot be as small as observed. Lampton *et al.* state that the parameter $\Delta\chi^2 = \chi^2 - \chi_{\min}^2$ should

be examined in order to determine the errors in these "best" values, and that $\Delta\chi^2$ is distributed as a chi-square variable with, in this case, two degrees of freedom. Figure 7 shows the resulting error figures in the (b, N) -plane corresponding to confidence levels of 68% ("one sigma") and 90%.

If one were interested in N alone, and regarded b as irrelevant, then examination of the minima in $\Delta\chi^2$ for each N at arbitrary b (a χ^2 variable with 1 degree of freedom) defines $N = 2.5 (+0.5, -2.2) \times 10^{15}$ (errors are 1σ , 68% confidence level). The corresponding range in which N lies with 90% confidence is 6.10^{13} – $4.10^{15} \text{ cm}^{-2}$. Conversely, examining b alone, and regarding N as irrelevant, gives $b = 9.8 (+2.2, -1.0) \text{ km s}^{-1}$ (again, 1σ errors) with b lying with 90% confidence in the interval 8.4 – 13.5 km s^{-1} .

The above values for the column of sodium atoms are high. The only available calibration between sodium column and visual absorption is through observations of stars in our Galaxy, which necessitates the heart-stopping assumptions that the sodium abundance, ionization balance, and dust-to-gas ratio are the same in the interstellar media of our Galaxy and IC 4329A. Using the values found by Morton (1975) for ζ Oph, namely, $A_v = 0.96 \text{ mag}$ for $\log N = 13.86$, it is found that IC 4329A, $A_v = 33 \text{ mag}$ (+7, -29), where the errors represent 1σ and A_v lies in the range 0.8 – 53 mag with 90% confidence. However, it is most unlikely that A_v should exceed 7 mag because IC 4329A would then be intrinsically more luminous than 3C 273 and its Balmer decrement difficult or impossible to understand. The visual absorption derived from the D-line study is best stated as $A_v > 1.6 \text{ mag}$ with 90% confidence. This value for A_v is in agreement with those derived from the Balmer decrement and the shape of the continuum. This absorption derived from the D lines refers, of course, to the continuum source rather than the line-emitting region.

The range of values of the velocity parameter b are also interesting. In our Galaxy, the values of b found in analyses of D-line ratios in stars seen through one or more spiral arms cluster around 9 km s^{-1} (Münch 1968). Thus we may conclude that noncircular motions in the disk of IC 4329A are small and that the velocity dispersion of its interstellar medium is quite comparable to that in our own Galaxy. This result is contrary to theoretical speculations that the interstellar media in Seyfert galaxies might be seriously disrupted. Evidently, the region in IC 4329A containing neutral sodium atoms has not been affected by the nuclear activity.

In retrospect, it seems that for IC 4329A the D lines may not be the ideal lines for this study. Possibly the H and K lines, which are seen in absorption in the low-dispersion data, would have been less saturated and provided a better estimate for A_v . Also, there are signs of the diffuse interstellar bands $\lambda\lambda 6180$ and 6283 in our data. Observations of H and K and of the Na I $\lambda\lambda 3302, 3303$ doublet, however, will be more difficult not only because IC 4329A is so red, but also because of the weakness of the lines. The continua of Seyfert galaxies and quasars are, in some ways, ideal for the

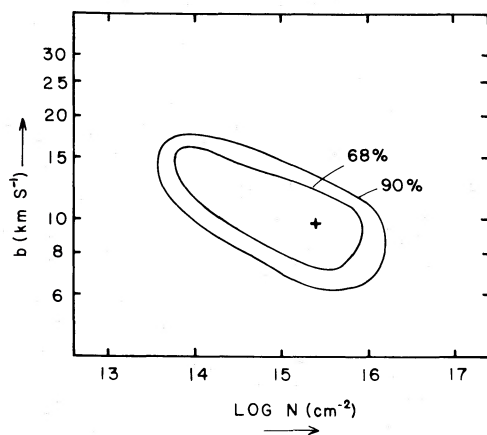


FIG. 7.—The best estimate (+) for the velocity parameter b and the column density N of neutral sodium atoms to the nucleus of IC 4329A, together with the 68% ("one sigma") and 90% confidence error figures plotted in the (b, N) -plane.

study of interstellar media, since they are bright and free of intrinsic, narrow spectral features. Extension of this method to determine the absorptions within other Seyfert galaxies and quasars is both possible and desirable.

d) Physical Conditions

In order to derive physical conditions in the forbidden-line region, the relative line intensities have been corrected (Table 2) by the reddening derived from the Balmer decrement ($A_v = 4.8$ mag, § IVa). Three line ratios may be used to estimate the electron density and temperature in IC 4329A:

1. [S II] 6731 Å/6717 Å. The electron density is found to be $N_e \approx 4900(T_e/10^4)^{1/2} \text{ cm}^{-3}$ (derived from parameters given in Saraph and Seaton 1970).

2. [S II] 4069 Å/6724 Å. N_e ranges between $2.2 \times 10^5 \text{ cm}^{-3}$, for $T_e = 4 \times 10^3 \text{ K}$, and $1.8 \times 10^4 \text{ cm}^{-3}$, for $T_e = 3 \times 10^4 \text{ K}$ (references for atomic parameters are Czyzak and Krueger 1963, Czyzak *et al.* 1970, and Saraph and Seaton 1970).

3. [O III] (4959 + 5007 Å)/4363 Å. This ratio is uncertain because of the difficulty of separating the $\lambda 4363.2$ line from $H\gamma$. If, however, loci from these three line ratios are plotted in the N_e versus T_e plane, they intersect at $N_e \sim 10^4 \text{ cm}^{-3}$ over the whole range of possible values for the intensity of $\lambda 4363.2$ (atomic parameters for O^{++} from Seaton 1975). The temperature at intersection ranges from 20,000 K (relative intensity $\lambda 4363.2 = 2.2$) to 10^5 K (relative intensity $\lambda 4363.2 = 7.3$, Table 2). However, if $\lambda 4363.2$ is strong, it seems more plausible that the temperature is lower and that the [O III] emission originates in a denser region than the [S II]. If T_e is taken to be 10^4 K , and the relative intensity of $\lambda 4363.2 = 7.3$, then $N_e = 6.9 \times 10^6 \text{ cm}^{-3}$ in the [O III] region, consistent with Disney's (1973) conclusion.

V. THE NUCLEAR LUMINOSITY OF IC 4329A

IC 4329A is clearly an extremely luminous Seyfert galaxy. By comparing our IDS spectra with those of standard stars observed on the same night, the flux in $H\beta$ is found to be $7 \times 10^{-13} \text{ ergs cm}^{-2} \text{ s}^{-1}$. This value is quite uncertain, perhaps by as much as a factor of 2, since it is determined by observation through a small entrance aperture. For $H_0 = 50 \text{ km s}^{-1} \text{ Mpc}^{-1}$, the $H\beta$ luminosity is $7 \times 10^{41} \text{ ergs s}^{-1}$ with no correction for absorption, or $1 \times 10^{44} \text{ ergs s}^{-1}$ after correction for $A_v = 4.8$ mag, as derived from the Balmer decrement (§ IVa). If $A_v \approx 2.5$ mag, the estimate from the continuum shape (§ IVb), this luminosity becomes $1 \times 10^{43} \text{ ergs s}^{-1}$. These values are close to those of many quasars (see, e.g., Weedman 1976). Using Disney's (1973) photometry through a $10''$ diaphragm, $V = 14.4$ mag, and taking A_v to lie between 2.5 and 4.8 mag, the absolute magnitude M_v lies in the range -23.0 to -25.3 , values typical of lower-luminosity quasars. Although only a weak radio source (M. J. Disney, quoted by de Bruyn and Wilson 1976), IC 4329A is the identification of the X-ray source 2A 1347-300 (Cooke *et al.* 1978; Delvaile, Geller, and Schnopper (1978) with X-ray luminosity in the 2-10 keV band $6.6 \times 10^{43} \text{ ergs s}^{-1}$ (Elvis *et al.* 1978). On the basis of its reddening-corrected optical nuclear luminosity, IC 4329A may be dubbed "the nearest quasar".

We are grateful to M. J. Disney for his interest in and stimulation of these results and to R. A. E. Fosbury and M. J. Ward for assistance in the acquisition of the data. D. C. Morton provided the curves of growth used in the analysis of the Na I D lines. We thank the U.K. Science Research Council (SRC) for allocation of observing time on the Anglo-Australian telescope and for travel finance.

REFERENCES

- Allen, C. W. 1973, *Astrophysical Quantities* (London: Athlone).
- Boksenberg, A. 1972, Proceedings of the ESO/CERN Conference on Auxiliary Instrumentation for Large Telescopes, Geneva, 1972 May 2-5, p. 295.
- Boksenberg, A. and Burgess, D. E. 1973, Proceedings of Symposium on Astronomical Observations with Television-Type Sensors, Vancouver, 1973 May 15-17, p. 21.
- Boksenberg, A., Carswell, R. F., Allen, D. A., Fosbury, R. A. E., Penston, M. V., and Sargent, W. L. W. 1977, *M.N.R.A.S.*, **178**, 451.
- Cooke, B. A., Elvis, M., Maccacaro, T., Ward, M. J., Fosbury, R. A. E., and Penston, M. V. 1976, *M.N.R.A.S.*, **177**, 121P.
- Cooke, B. A., *et al.* 1978, *M.N.R.A.S.*, **182**, 489.
- Czyzak, S. J., and Krueger, T. K. 1963, *M.N.R.A.S.*, **126**, 177.
- Czyzak, S. J., Krueger, T. K., Martins, P. de A. P., Saraph, H. E., and Seaton, M. J. 1970, *M.N.R.A.S.*, **148**, 361.
- de Bruyn, A. G., and Wilson, A. S. 1976, *Astr. Ap.*, **53**, 93.
- Delvaile, J. P., Geller, M. J., and Schnopper, H. W. 1978, *Ap. J. (Letters)*, **226**, L69.
- Disney, M. J. 1973, *Ap. J. (Letters)*, **181**, L55.
- Elvis, M., Maccacaro, T., Wilson, A. S., Ward, M. J., Penston, M. V., Fosbury, R. A. E., Perola, G. C. 1978, *M.N.R.A.S.*, **183**, 129.
- Lampton, M., Margon, B., and Bowyer, S. 1976, *Ap. J.*, **208**, 177.
- Martin, W. L. 1974, *M.N.R.A.S.*, **168**, 109.
- Moore, C. E. 1972, *A Multiplet Table of Astrophysical Interest*, National Bureau of Standards, Washington, D.C.
- Morton, D. C. 1975, *Ap. J.*, **197**, 85.
- Morton, D. C., and Smith, W. H. 1973, *Ap. J. Suppl.*, **26**, 333.
- Münch, G. 1968, in *Stars and Stellar Systems*, Vol. 7, ed. B. M. Middlehurst and L. H. Aller (Chicago: University of Chicago Press), p. 365.
- Oke, J. B., 1974, *Ap. J. Suppl.*, **27**, 21.
- Osterbrock, D. E. 1974, *Astrophysics of Gaseous Nebulae* (San Francisco: W. H. Freeman).
- Osterbrock, D. E. 1977, *Ap. J.*, **215**, 733.
- Penston, M. V., and Fosbury, R. A. E. 1978, *M.N.R.A.S.*, **183**, 479; erratum, **186**, 603.
- Phillips, M. M. 1976, *Ap. J.*, **208**, 37.
- Robinson, L. B., and Wampler, E. J. 1972, *Pub. A.S.P.*, **84**, 161.
- . 1973, in *Astronomical Observations with Television-Type Sensors*, ed. J. W. Glaspey and G. A. H. Walker. (Vancouver: University of British Columbia Press).
- Saraph, H. E., and Seaton, M. J. 1970, *M.N.R.A.S.*, **148**, 367.
- Seaton, M. J. 1975, *M.N.R.A.S.*, **170**, 475.
- Strömgren, B. 1948, *Ap. J.*, **108**, 242.
- Weedman, D. W. 1976, *Ap. J.*, **208**, 30.
- Whitford, A. E. 1958, *Astr. J.*, **63**, 201.

A. S. WILSON: Astronomy Program, University of Maryland, College Park, MD 20472

M. V. PENSTON: ESA Villafranca del Castillo Satellite Tracking Station, P.O. Box Apartado 54065, Madrid, Spain